UNIVERSITYOF BIRMINGHAM

Fragility function development and seismic loss assessment of expansion joints

Otsuki, Yu; Kurata, Masahiro; Skalomenos, Konstantinos; Ikeda, Yoshiki

[Link to publication on Research at Birmingham portal](#)

FRAGILITY FUNCTION DEVELOPMENT AND SEISMIC LOSS ASSESSMENT OF EXPANSION JOINTS

Journal:	*Earthquake Engineering and Structural Dynamics*
Manuscript ID	Draft
Wiley - Manuscript type:	Research Article
Date Submitted by the Author:	n/a
Complete List of Authors:	Otsuki, Yu; Kyoto University, Graduate School of Engineering Kurata, Masahiro; Kyoto University, Disaster Prevention Research Institute Skalomenos, Konstantinos; Kyoto University, Disaster Prevention Research Institute Ikeda, Yoshiki; Kyoto University, Disaster Prevention Research Institute Akazawa, Motoki; Takenaka Corp, Structural Engineering Section
Keywords:	Expansion joints, Non-structural components, Fragility function, Relative displacement, Adjacent buildings

FRAGILITY FUNCTION DEVELOPMENT AND SEISMIC LOSS ASSESSMENT OF EXPANSION JOINTS

Yu Otsuki[1], Masahiro Kurata[2], Konstantinos A. Skalomenos[2], Yoshiki Ikeda[2], and Motoki Akazawa[3]

[1]Graduate School of Engineering, Kyoto University, Kyoto-shi, Kyoto, 615-8530, Japan,
otsuki.yu.65n@st.kyoto-u.ac.jp, corresponding author
[2]Disaster Prevention Research Institute, Kyoto University
[3]Structural Engineering Section, Takenaka Corporation

Expansion joints connecting adjacent buildings accommodate relative motions generated by wind, thermal or earthquake loads but often exhibit damage during severe earthquakes. However, the level of damage and safety factor required to avoid loss of function are not well considered in the current design practice. The objective of this paper is to provide quantitative information on the seismic damage probability of common expansion joints and the associated repair cost so that designers can refer as a decision basis in the selection of expansion joints. Four commonly used types, high- and standard-performance floor and wall expansion joints, whose damage states have been evaluated recently by the authors through shake table testing, are considered. First, the fragility functions of expansion joints for seven damage patterns are developed utilizing the test results. Next, the vulnerability of the expansion joints installed between adjacent buildings is assessed by incremental dynamic analysis and the recommended level of the safety factor to ensure the function of expansion joints is discussed. In the end, a procedure for cost-effective selection of expansion joints is introduced and the dependency of the appropriate selection of expansion joints on building characteristics is demonstrated in case studies. The presented results are deemed to be beneficial for improving the design practice of expansion joints and reducing future seismic loss.

KEYWORDS

Expansion joints, Non-structural components, Fragility function, Relative displacement, Adjacent buildings

1   INTRODUCTION

Decisions regarding the design of buildings in seismic regions are often made in terms of the risk expected in the building lifespan. Damage of non-structural components caused by an earthquake results in significant economic loss, which can exceed the replacement cost of the building [Sullivan et al. 2018]. Nonstructural damage also causes serious injuries and economic loss but current seismic design methodologies consider nonstructural damages indirectly by checking drift limits and floor acceleration. For the risk assessment, the fragility functions of various building components and associated information on repair cost, procedure, and time are necessary [Skalomenos KA et al. 2015]. The Federal Emergency Management Agency (FEMA) provides such information for wide variety of structural and non-structural components and the Applied Technology Council (ATC) developed an electronic Performance Assessment Calculation Tool (PACT) to perform the probabilistic computations and accumulation of losses [FEMA 2012].

Expansion joints connecting adjacent buildings accommodate relative motions generated by wind, thermal or earthquake loads but often exhibit damage during severe earthquakes. However, the damage limit states of expansion joints and safety factor required to avoid failure are not well considered in the current design practice. In addition, the fragility information for expansion joints has not been prepared yet and the vulnerability and seismic loss analysis of expansion joints are not available. Expansion joints at apartment buildings dropped off during the 2005 Fukuoka earthquake [AIJ 2005] and the 2016 Kumamoto earthquake [NILIM and BRI 2016], and 90 of 327 expansion joints at base-isolated buildings were heavily damaged during the 2011 Tohoku earthquake [Kasai et al. 2013]. Seismic poundings between adjacent buildings have been observed in past earthquakes, which could result in significant damage to expansion joints [Bertero et al. 1986, Filiatrault et al. 1994, Kasai et al .1997, and PWRI 1997, and Cole et al. 2012]. Especially after the 2011 Tohoku earthquake, building owners are more concerned on the seismic performance of non-structural components considering their impacts on the building serviceability and risk management [AIJ 2013]. In phase with these campaigns, the guidelines of expansion joints have been recently published by the Japanese Society of Seismic Isolation (JSSI) [JSSI 2013], and the Japan Expansion Joint Association (JEJA), an association consisting of six expansion joint manufacturers [JEJA 2016]. These guidelines discuss the basic behavior, damage states and testing of expansion joints within the design motion range, but the behaviors beyond the design motion range are not well addressed.

The typical seismic design of expansion joints connecting adjacent buildings is shown in Figure 1(a), where the key design parameters are i) the minimum separation distance between the buildings, ii) the safety factor, and iii) the motion range of expansion joints. Figure 1(b) illustrates the definition of each parameter for a typical floor expansion joint. Seismic codes prescribe a minimum separation distance between two buildings for avoiding seismic pounding and provide simplified computation methods of the peak relative displacement [BCJ 2008, ICBO 1997, CEN 2005, and TBC 1997]. For

a performance-based design framework, a probabilistic analysis procedure for computing seismic pounding risk has been recently developed [Tubaldi 2016]. A safety factor is selected by structural engineers to determine the clearance between adjacent buildings; the clearance is calculated as the product of the minimum separation distance and the safety factor. The value of safety factor is vaguely determined by structural engineers due to the lack of a quantitative relation between the safety factor and performance. The design motion range of expansion joints, defined as the ratio to the clearance between two buildings, typically ranges from 20% to 80% [JEJA 2016]. When this ratio is smaller than the reciprocal of safety factor, there is a possibility of damage to the expansion joints, even against code-level ground motions. As pointed out by [Kasai et al. 2013], one of the major causes of damage to expansion joints in the 2011 Tohoku earthquake was an insufficient motion range. Therefore, the quantitative evaluation of safety factor and damage to expansion joints is necessary to provide a basis for decision makers in the design process.

Regarding the capacity of expansion joints, there are several performance levels in Japan. JSSI [JSSI 2013] defines three seismic performance ranks, A, B and C, in expansion joints for base-isolated buildings. JFJA [JFJA 2016] issues a guideline that explains the basic behavior and damage states of expansion joints for general buildings referring the desirable performance of the expansion joints to the recommendations for seismic design and the construction of non-structural components [AIJ 2003]. To investigate the difference of seismic performances and damage patterns of various expansion joints, the authors have conducted shaking table tests for four commonly used types, high-performance (HP) and standard-performance (SD) floor and wall expansion joints. Totally seven damage patterns were observed and the critical relative displacement that initiates each damage state was identified. As expected, the HP expansion joints showed better seismic performance than the SD expansion joints that failed immediately after the motion range [Otsuki et al. 2018a]. These results suggest that the extent of safety factor to be considered in the design process should be different for various performance levels of expansion joints.

The objective of this paper is to evaluate the vulnerability and seismic loss of expansion joints for different seismic performance levels and safety factors so that designers can refer as a quantitative basis in the selection of expansion joints. First, the fragility functions of expansion joints were developed by using the available test data. Then, the vulnerability and seismic loss analysis were conducted using two sets of adjacent buildings models. One set consisted of a 55-story super high-rise and 13-story high-rise and the other set consisted of two 13-story high-rise buildings. Using the results of incremental dynamic analyses and the developed fragility functions, the relationship between a safety factor and damage probability of the expansion joints was investigated. The presented results on the vulnerability and repair cost for expansion joints of various performance levels and safety factor offer structural designers and building owners a quantitative decision basis in the selection of expansion joints.

2 DAMAGE PATTERNS OF EXPANSION JOINTS OBSERVED IN SHAKE TABLE TESTS

This section overviews the behavior and damage states of the expansion joints observed in the shake table tests conducted by the authors [Otsuki et al. 2018a]. Table 1 summarizes the deformation mechanisms, drawings and damage states of the expansion joints. The HP expansion joints were for base-isolated buildings and conformed to rank A [JSSI 2013]. These types were custom-made. The SD specimens were widely used for general buildings and off-the-shelf. Expansion joints were set between two steel frames with fundamental periods of 6.0 s and 0.46 s. Ground motions and sine waves were applied in the X-direction. Sequential damage to the expansion joints was simulated by sine waves of 1 Hz with amplitude increased from 300 cm/s^2 to the failure of the expansion joints by the 50 cm/s^2 increment. The nominal motion range of the expansion joints in the horizontal directions was 17.5 cm, which corresponds to 50% of the clearance. Totally seven damage patterns were observed and classified into damage states defined by [JSSI 2013]. Damage state 1 (DS1) and failure were sequential damage, and DS-1A and DS-1B were simultaneous damage [Porter et al 2007]. Most of the damage patterns were displacement dependent, and therefore the critical relative displacement that initiates each damage state was presented. Brief descriptions of each expansion joint and their damage states are presented here.

2.1 HP floor expansion joint

The deformation mechanism of the HP floor expansion joint was a sliding type. Most of the parts of the expansion joint were made of steel. The cover plate was not fixed in the Z-direction, thus permitting vertical deformation. Expansion joints for base-isolated buildings must hold a central restoring device to avoid a residual displacement [JSSI 2013], and this expansion joint holded a bellows-shaped mechanism for this role.

One damage state 1 was observed where the cover plate was disengaged due to the collision when the two frames got closer. This damage is easily fixed by relocating the cover plate to the original position. The critical relative displacement was nearly 200% of the motion range of 17.5 cm, showing its high seismic capacity.

2.2　HP wall expansion joint

The HP wall expansion joint had a lifting deformation mechanism. The cover plate was lifted when the expansion joint was subjected to displacement in the Y-direction or compressive displacement in the X-direction, but the springs pulled back the cover plate to the original position after an excitation. This expansion joint was also made of steel.

Two damage states DS1-A and DS1-B were observed. One was that three of five springs inside the cover plate were caught on a surrounding member at the time of compression, and a residual deformation remained in the spring. The other damage was the rupture of screws at the base material due to the impact force applied when a collision occurred. The critical relative displacement of both damage patterns was nearly equal to 110 and 130% of the design motion range.

2.3　SD floor expansion joint

The deformation mechanism of the SD floor expansion joint was categorized a sliding type. It consisted of an unfixed center cover plate with side plates made of stainless steel. Rubber sheets were fixed in between the cover plate and side plates. There were a total of twenty drill screws at the side plates. This expansion joint exhibited a residual displacement after an excitation because there was no center-restoring mechanism.

DS1 was the rupture of screws. When two frames approached, the cover plate hit the screws several times, resulting in bending and fracture. When a large relative displacement applied, the cover plate was disengaged from the side plate. The cover plate could no longer sustained human weight and its function was lost. This damage was classified as failure. DS1 occurred within the motion range and the failure occurred at approximately 130% of the motion range.

2.4　SD wall expansion joint

The deformation mechanism of the SD wall expansion joint was rail sliding type. The cover plate was equipped with four sliders that permit deformation in the X-direction. The length of the slider was 17.5 cm. All plates and sliders were made of aluminum. The rubber sheets were equipped between the cover plate and surrounding materials.

DS1 was the disengagement of the rubber sheets due to rubbing with surrounding components during excitations. This damage led to concern about air and water leakage. This damage was resulted from repeated loading during shakings, and therefore it is difficult to identify the critical demand value that initiates this damage. When relative displacement reached just beyond the motion range, the cover plate dropped off because its sliders railed off. This damage was classified as failure because its function was lost.

3　DEVELOPMENT OF FRAGILITY FUNCTIONS FOR EXPANSION JOINTS

3.1　Fragility functions for displacement dependent damage

This section presents the development of the component fragility functions for the expansion joints using the test results. A fragility function expresses the probability of being in or exceeding a damage state (*DS*) as a function of an engineering demand parameter (*EDP*). The cumulative lognormal distribution is typically used to define a fragility function [Porter et al. 2007]. Eq. (1) expresses a fragility function, where $\Phi()$ is the standard normal cumulative distribution function, and $\theta_{c,i}$ and $\beta_{c,i}$ are the median and standard deviation of the natural logarithm of the capacity to resist damage state ds_i.

$$P[DS \geq ds_i \mid EDP = edp] = \Phi\left(\frac{\ln edp - \ln \theta_{c,i}}{\beta_{c,i}}\right) \tag{1}$$

For sequential damage, the probability of being in a specified damage state $DS = ds_i$ given $EDP = edp$ is expressed by:

$$P(ds_i \mid edp) = \begin{cases} P[DS \geq ds_i \mid edp] - P[DS \geq ds_{i+1} \mid edp] & 1 \leq i < n \\ P[DS \geq ds_i \mid edp] & i = n \end{cases} \tag{2}$$

where $n = 2$ in this study with $ds_1 = $ DS1 and $ds_2 = $ Failure.

To develop fragility functions, various methods have been proposed. Especially for the displacement sensitive damage, i.e. the case of expansion joints, [FEMA 2012] recommends a following methodology to develop fragility functions: "The median displacement demand at initiation of failure should be taken as the calculated available length of travel based on the specified travel allowance dimension. The dispersion should be estimated based on the likelihood that the initial position of the structure is out of tolerance. Normal construction tolerances can be considered as representing one standard deviation on the displacement dimension. The dispersion can then be taken as equal to the coefficient of variation, which is approximated by the standard deviation value (i.e., construction tolerance), divided by the median (i.e., travel allowance dimension)". Considering the above descriptions and the available test data, the procedure for developing fragility functions of expansion joints is summarized as follows:

·　Define the median $\theta_{c,i}$ as a critical length in a design paper or as a critical measurement value obtained by the experiment.

- Define the dispersion $\beta_{c,i}$ dividing the initial position errors expected in expansion joints by the travel allowance dimension if it is totally displacement sensitive damage or follow the value recommended by [FEMA 2012].

3.2 Initial position errors of expansion joints

The initial position of expansion joints may contain four inherent errors: construction error, dry expansion and contraction, heat expansion and contraction, and residual displacement. The expected maximum value for each error of expansion joints for base-isolated buildings is provided by [JSSI 2010] as listed in Table 2. Because these values are for expansion joints for base-isolated buildings, a small change is required when it is applied to the SD expansion joints used in the test, which is not commonly used for base-isolated buildings. The difference in the mechanism between expansion joints for isolation buildings and for other buildings is a center restoration capability. The expected residual displacement of the SD expansion joints was more than 1.0 cm based on the test observation by the authors, or 3.0 cm by engineering judgement.

The probability distribution of each error was assumed to follow a normal distribution with zero mean and the maximum error value in Table 2 as three standard deviations. Thus, the total standard deviation for the HP expansion joints, noted by σ_{HP}, was calculated as 0.83 cm and that for the SD expansion joints, noted by σ_{SD}, was 1.26 cm.

3.3 Fragility functions for expansion joints

Table 3 presents the fragility functions of the expansion joints for the described seven damage patterns. A dash line in each fragility function indicates the design motion range, noted by D_{expj}, equal to 17.5 cm. The small dots express relative displacements measured in each input. The dots at the probability equal to 0 indicate the peak relative displacement measured during each input before the damage occurrence. The dots at the probability equal to 1 indicate the relative displacement at the exact moment of damage (i.e. critical relative displacement in Table 1) described in [Otsuki et al. 2018a]. The detail of each fragility function is explained in below.

3.3.1 *HP floor expansion joint DS1: cover plate relocated*

In the test, the cover plate of the HP expansion joint was relocated due to a collision between the cover plate and side plate. The critical relative displacement for this damage was 33.8 cm, which was nearly equal to 200% of the design motion range of 17.5 cm (33.8 / 17.5 = 1.92). Therefore, the median value was adopted as $\theta_{c,i} = 2.0 D_{expj} = 35.0$ cm. A large dispersion must be considered because the collision does not always occur even when the relative displacement reached to 33.8 cm [Otsuki et al. 2018a]. When constructing a fragility function having such large uncertainty, FEMA suggests to use dispersion $\beta_{c,i} = 0.4$. However, with $\beta_{c,i} = 0.4$ this damage could happen even within the design motion range as shown in Table 3, and this does not make sense with the test results. Therefore, $\beta_{c,i} = 0.25$ is adopted so that the damage probability at the design value equals zero.

3.3.2 *HP wall expansion joint DS1-A: spring deformation*

Residual displacements of some of the five springs of the HP wall expansion joint were observed after a surrounding component collided with the springs. Table 4 lists the maximum relative displacement on the compression side and the number of damaged springs during each input. The critical relative displacement for this damage state was uncertain [Otsuki et al. 2018a] and the maximum relative displacement for each input was used to calculation the median and dispersion. Following the procedure in [FEMA 2012], the median $\theta_{c,i} = 22.0$ cm and the dispersion $\beta_{c,i}' = 0.086$ were obtained. In the case for five or fewer specimens, it is recommended to increase the dispersion by 0.25 [FEMA 2012]. Thus the total dispersion $\beta_{c,i}$ was obtained as 0.265.

$$\theta_{c,i} = \exp\left(\frac{1}{n_i} \sum_{i=1}^{n_i} \ln(r_i) \right) = \exp\left(\frac{\ln(19.1) + \ln(23.6) + \ln(23.6)}{3} \right) = 22.0\,\text{cm} \tag{3}$$

$$\beta_{c,i}' = \sqrt{\frac{1}{n_i - 1} \sum_{i=1}^{n_i} \left(\ln(r_i / \theta_{c,i}) \right)^2} = 0.086 \tag{4}$$

$$\beta_{c,i} = \sqrt{0.086^2 + 0.25^2} = 0.265$$

3.3.3 *HP wall expansion joint DS1-B: screw rupture*

The several screws of the HP wall expansion joint were damaged by a large impact force applied when the two frames had a collision. Therefore, the distance between the collision points, noted by a, is critical for this damage and the median value

was set as $\theta_{c,i} = a = 21.0$ cm. The dispersion $\beta_{c,i} = 0.04$ was obtained by dividing the standard deviation of initial position errors σ_{HP} by the median capacity $\theta_{c,i} = 21.0$ cm.

3.3.4 *SD floor expansion joint DS1: screw rupture*

The damage to screws depends on the length of the cover plate and screws as noted *a* in Table 3. The test results confirmed that the collision between the cover plate and screws was likely to occur when the relative displacement reached to a half of the expected collision distance 2*a* due to the imbalance of the friction coefficient of the rubber sheets [Otsuki et al. 2018a]. Thus, the median value of this damage state was taken as $\theta_{c,i} = a = 9.6$ cm. The screws were ruptured after repeated collisions. Therefore, a large dispersion should be considered and we adopted $\beta_{c,i} = 0.4$ proposed by [FEMA 2012] for a case with large uncertainty. Note that the dots are excluded in Table 3 because the fracture of the screws occurred after several collisions.

3.3.5 *SD floor expansion joint Failure: cover plate disengaged*

The disengagement of the cover plate of the SD floor expansion joint depends on the dimensions *a* and *b* of the cover plate in Table 3. The critical relative displacement measured in the test was 22.2 cm, which equaled nearly 2 (*a* + *b*) = 22.6 cm. Therefore, this value was taken as the median value. The dispersion $\beta_{c,i} = 0.056$ was obtained by dividing the standard deviation of the initial position errors σ_{SD} by the median capacity $\theta_{c,i} = 22.6$ cm.

3.3.6 *SD wall expansion joint DS1: rubber sheet disengaged*

The rubber sheet of the SD wall expansion joint was disengaged due to the repeated rubbing with surrounding materials during shakings. This damage state cannot be totally displacement-dependent, but assumed here that as same as other damage states. This damage state was not observed after the input of 300 cm/s² and 350 cm/s², but observed after the input of 400 cm/s². The peak relative displacements during the excitation of 300 cm/s² and 350 cm/s² were 15.3 cm and 15.1 cm, which equaled nearly 85% of the motion range. Thus, the median value was taken as $\theta_{c,i} = 0.85D_{expj} = 14.9$ cm. Considering the large uncertainty of the occurrence of this damage, $\beta_{c,i} = 0.40$ was set following [FEMA 2012].

3.3.7 *SD wall expansion joint Failure: cover plate dropped off*

The test results showed that the cover plate of the SD wall expansion joint dropped off exactly when the relative displacement exceeded the slider length. Thus, the median value was taken as the slider length $\theta_{c,i} = a = 17.5$ cm. The dispersion $\beta_{c,i} = 0.072$ was obtained by dividing the standard deviation of the initial position errors σ_{SD} by the median capacity $\theta_{c,i} = 17.5$ cm.

4 ADJACENT BUILDING MODEL

Damage to expansion joints depends on the peak relative displacement and the peal relative displacement between adjacent buildings depends on building characteristics such as fundamental periods, damping ratios, and the type of force-displacement hysteresis curves [Kasai 1996, Tubaldi 2015]. To see the effect of building characteristics on the selection of expansion joints, two representative sets of adjacent buildings in urban cities are prepared in this study as shown in Figure 2. One adjacent building model consists of a 55-story super high-rise building and a 13-story high-rise building. This is called SH model (Super high-rise and High-rise). A skyscraper and a high-rise building are often connected in a city center for convenience of building users. The other adjacent building model consisted of two 13-story high-rise buildings. This is called HH model (High-rise and High-rise). Due to height restrictions, high-rise buildings of the same height often line up in urban developing areas. For both sets of adjacent buildings, a sky bridge with the tested expansion joints is assumed at a height of 44 m. This height is equivalent to the 9th floor height of the 55-story building and the 12th floor height of the 13-story building. Sky bridges are usually installed as a cantilever hanged from one building and expansion joints are installed at the end of the other building. The expansion joints and sky bridge are not considered in the modeling as they do not resist against deformation and contribute much to the dynamic behavior of the models.

The 55-story super high-rise building is a 238-m-high steel structure with 55 stories above (54 floor and roof) and 6 stories below ground level. The spread foundation is designed to be secured over the bedrock layer at a depth of around 30 m. The first natural period is 5.79 s. The structural system of the building is a set of steel moment-resisting frames with oil dampers and buckling-restrained braces. More detail information and results of seismic response analysis can be found in [Otsuki et al. 2018b]. The 13-story high-rise building is a 52-m-high steel structure with buckling-restrained braces. It has 13 stories above ground and 1 story underground. The first natural period is 1.37 s. Both buildings were designed to satisfy the current Japanese building code. SH model consists of these two buildings.

HH model is composed of the described 13-story building and its adjusted 13-story building. The periods of the adjacent buildings with the same heights are generally not equal due to the different characteristics of buildings such as mass and stiffness [Lin and Weng 2001]. Therefore, the adjusted 13-story building was created by multiplying each floor mass of the

original 13-story building by 1.2. The natural period of the adjusted 13-story building is 1.50 s. The locations of the SH model and HH model are assumed in Tokyo, Japan.

From the structural design information, shear models for buildings were created in OpenSees [PEER 2016]. The structural elements were reduced to a 61 degree-of-freedom system (55 stories above ground and 6 stories underground) and 14 degree-of-freedom system (13 stories above ground and 1 story underground) with lumped mass, respectively. The stiffness of each story above ground was represented by a shear spring with a normal trilinear force-deformation hysteresis curve. The shear springs of underground stories were considered to be elastic. The internal viscous damping was set to 1% of the critical level at the first natural period for the 55-story building and 2% for the 13-story buildings, and their matrices were proportional to the initial stiffness matrices. For the 55-story building, a Maxwell damper model was connected in series on each story to consider the oil dampers. For both models, the springs with negative stiffness were inserted to capture large P-Delta effects in the shear model [Akiyama 2007]. For SH model and HH model, the soil amplification factor was not considered and input ground motions were applied at the base of the underground story.

5 VULNERABILITY ASSESSMENT OF EXPANSION JOINTS

5.1 Intensity measure

In this section, the vulnerability of the expansion joints installed on the adjacent building models is assessed by incremental dynamic analysis (IDA). The appropriate safety factor for each expansion joint and for each adjacent building model is recommended using the results. Under the framework in performance-based earthquake engineering, IDA is often used to quantify the relationship between EDP and intensity measure (IM) [Vamvatsikos et al. 2002]. For IDA, the appropriate IM is essential to reduce the computational cost and variance of response. Commonly used IMs are PGA, PGV, and spectral acceleration at the fundamental period [Biasio et al. 2015]. However, in the case for expansion joints where damage depends on the peak relative displacement between two buildings, IM should be sensitive to the peak relative displacement. [Tubaldi et al. 2016] studied on the selection of the appropriate intensity measure for the seismic pounding problem between two buildings and proposed the following intensity measure, noted by IM_{rel}:

$$IM_{rel} = \gamma_A S_d(T_A)\sqrt{1 + R^2 - 2\rho R}$$

$$R = [\gamma_B S_d(T_B)]/[\gamma_A S_d(T_A)]$$

$$\rho = \frac{8\sqrt{\zeta_A \zeta_B}\left(\zeta_A + \zeta_B \frac{T_A}{T_B}\right)\left(\frac{T_A}{T_B}\right)^{1.5}}{\left[1 - \left(\frac{T_A}{T_B}\right)^2\right]^2 + 4\zeta_A\zeta_B\left[1 + \left(\frac{T_A}{T_B}\right)^2\right]\left(\frac{T_A}{T_B}\right) + 4\left(\zeta_A^2 + \zeta_B^2\right)\left(\frac{T_A}{T_B}\right)^2} \tag{5}$$

where $S_d(T)$ denotes the spectral displacement at the fundamental period T of the building, and γ denotes the participation factor of the fundamental mode. When computing γ, the modal shape must be normalized to have a unit displacement at the pounding location. ρ expresses the correlation factor between two buildings with parameters of the fundamental period T and damping ratio ζ. In summary, IM_{rel} estimates the peak relative displacement by considering the peak displacements and phase difference of two buildings. The correlation factor ρ is 0.000327 for SH model and 0.163 for HH model. The participation factors of two buildings at the location of the expansion joints are 0.228 for the 55-story building and 1.26 for the 13-story building.

5.2 Motion range of expansion joints

The motion range of the expansion joints for SH model and HH model is set as listed in Table 5. In Japan, the minimum separation distance is calculated by time history analysis or set as the absolute sum (ABS) of the peak displacements of two buildings from modal response analysis against the Level 2 seismic hazard spectrum [BCJ 2008]. The return period of the Level 2 seismic hazard is approximately 500 years and the Level 2 design acceleration spectrum is presented in Figure 3.

In general, the ABS rule gives an overly conservative peak relative displacement especially when the fundamental periods of two buildings are close [Jeng 1992]. For example, the peak relative displacement estimated by the ABS rule is 39.5 cm for SH model and 46.9 cm for HH model, whereas the average of the peak relative displacements against 10 ground motions fitted to the Level 2 spectrum from time history analysis was 41.5 cm for SH model and 24.3 cm for HH model. The ABS rule gives a good estimation for SH model but a significantly overestimation for HH model. This is because the ABS rule does not consider the phase difference between two buildings, and the effect of the in-phase motions on the peak relative displacement is large for buildings with similar characteristics. The IM_{rel} value for the Japanese Level 2 spectrum is 36.5 cm for SH model and 30.4 cm for HH model. In contrast to the ABS rule, the IM_{rel} value gives a good estimation for

HH model. In this study, therefore, the minimum separation distance is set as the IM_{rel} value to avoid the overestimation by the ABS rule and because of its computational efficiency compared to time history analysis.

To reduce the number of parameters for comparison, this study fixes the motion range of the expansion joints as 50% of the clearance same as the test specimens. Thus, safety factor is the only parameter. The values of safety factor to be considered are 1.2, 1.5, and 1.8, and the corresponding clearance and design motion ranges are obtained as listed in Table 5. Since the fragility functions defined in the previous section were for the motion range of 17.5 cm, the median $\theta_{c,i}$ and dispersion $\beta_{c,i}$ related to the motion range for each fragility function used in the following sections were scaled by the corresponding motion range.

5.3 Incremental dynamic analysis

For the selection of input ground motions, this study adopts the 'Far Field' ground motions provided by [FEMA 2009]. This is because these ground motions have large magnitudes, PGA, PGV and wide range of frequency contents. In this study, the ground motions measured by the instruments whose effective period was less than 6 s were excluded from the original set because the fundamental period of the 55-story building is 5.79 s. From the PEER NGA database [PEER 2017], 30 ground motions (15 record station × 2 lateral directions) were obtained. Figure 3 displays the acceleration response spectra of 30 ground motions along with the Japanese Level 2 design spectrum with 2% damping ratio.

The selected 30 ground motions were scaled in accordance with IM_{rel} from 1 to 50 cm with the 1 cm increment and applied to the adjacent building models. For each simulation, the peak relative displacement at the location of expansion joints was taken out and the relationship between IM_{rel} and the peak relative displacement was obtained as displayed in Figure 4. There are several notable trends in this figure. At first, the reduction of the peak relative displacement can be seen in the range of large IM_{rel} values when the buildings undergo inelastic region. This is because the phase difference of the two buildings decreased by the hysteresis damping applied in the inelastic range as discussed in the previous study [Kasai et al. 1996]. Secondly, the reduction of the peak relative displacement is much larger for HH model. This can be assumed that HH model behaved more similarly in the nonlinear range than in the linear range due to the period elongation of one's building as discussed in [Tubaldi et al. 2016]. Third, the dispersion of the peak relative displacement increases after the buildings undergo inelastic range. This can be attributed to the fact that the IM_{rel} value predicts the peak relative displacement for elastic systems [Tubaldi et al. 2016]. Note that the inelastic behavior of the two buildings does not always reduce the peak relative displacement compared with the elastic system. There is a case that the peak relative displacement increases as the increase of IM_{rel} levels when the two buildings have the same behavior in the elastic range, but different yield displacements and nonlinear behaviors. Such behavior was reported in [Tubaldi et al. 2015].

Note that, in this IDA, the maximum scaling of the original ground motions was 6.15 for SH model and 6.73 for HH model. It is known that a large scaling of original recorded ground motions is not appropriate considering the different properties of ground motions for different levels of intensity measure [Baker and Cornell 2005]. Thus, other study [Tubaldi el al. 2016] conducted cloud analysis instead of IDA to derive the relationship between the peak relative displacement and IM_{rel} by using a set of 240 unscaled ground motions selected by [Baker et al. 2011]. However, these ground motions were selected in the period range up to 5 s, which is shorter than the fundamental period of the 55-story super high-rise building. Thus, these ground motions were not used in this study. Moreover, the probability of exceedance of seismic pounding obtained from cloud analysis with bilinear regression and from IDA showed a good match although the large scaling of original ground motions was adopted in IDA [Tubaldi et al. 2016].

5.4 Vulnerability assessment of HP and SD expansion joints

The probability of a component being in or exceeding certain damage state $DS = ds_i$ for a given level of a ground motion intensity measure $IM = im$ can be obtained by a similar manner to Eq. (1):

$$P[DS \geq ds_i \mid IM = im] = \Phi\left(\frac{\ln im - \ln \theta_{DS\mid IM}}{\beta_{DS\mid IM}}\right) \qquad (6)$$

and, the probability of being in $DS = ds_i$ given $IM = im$ is expressed by:

$$P(ds_i \mid im) = \begin{cases} P[DS \geq ds_i \mid im] - P[DS \geq ds_{i+1} \mid im] & 1 \leq i < n \\ P[DS \geq ds_i \mid im] & i = n \end{cases} \qquad (7)$$

For the estimation of $\beta_{DS\mid IM}$ and $\theta_{DS\mid IM}$ in Eq. (6), a regression analysis to the sufficient number of EDP- IM plots is required and this can be achieved by IDA. In general, the $EDP - IM$ relationship can be approximated by the linear regression in log-log dimension when systems are in elastic range. However, when $IM = IM_{rel}$ and EDP = peak relative displacement between two buildings, the linear regression cannot capture the change of the structural responses induced by the structural yielding and the bilinear regression is more accurate [Tubaldi et al. 2016]. Thus, this study also approximates the $EDP - IM$ relationship by the bilinear regression in log-log dimension.

Figure 5(a) demonstrates the parameters of the bilinear regression analysis, where $\ln a_1$ and $\ln a_2$ are the y-segments, b_1 and b_2 are the slopes of the lines, and $\ln im^*$ is the breakpoint of the two lines. The parameters of $\ln a_1$, b_1, b_2, and $\ln im^*$ for

the approximation of the *EDP – IM* relationship can be estimated by nonlinear least square regression. Figure 5(b) shows the bilinear regression curves for SH model and HH model by using the IDA results. For SH model, the bilinear curve was approximately linear. This is because the in-phase motion of the two buildings was less induced by the structural yielding. For HH model, the effect of the yielding was significant and the bilinear regression provided good match.

Table 6 lists the parameters to calculate Eq. (6) derived by combining the equations in [Padgett et al. 2008, Tubaldi et al. 2016]. These parameters are obtained from the regression parameters of $\ln a_1$, b_1, b_2, and $\ln im^*$ and have different values before and after the breakpoint im^*. At first, the dispersion of the *EDP* condition upon the *IM*, noted by $\beta_{EDP|IM}$, is obtained using the regression parameters as in Table 6. The total dispersion $\beta_{DS|IM}$ in Eq. (6) can be obtained by using $\beta_{EDP|IM}$, $\beta_{c,i}$ from the developed fragility functions of expansion joints, and the regression parameters. Finally, $\theta_{DS|IM}$ in Eq. (6) is calculated by using the regression parameters and the median capacity of the developed component fragility functions $\theta_{c,i}$, and Eq. (6) and Eq. (7) can be derived. Note that, the SD wall expansion joints have two fragility functions corresponding to DS1 and failure state. These fragility functions produce a negative probability of being in a certain damage state under Eq. (1). Thus, Eq. (1) for DS1 of the SD wall expansion joint was replaced with Eq. (8) as suggested by [Porter et al. 2007] so that each fragility function does not cross.

$$P[DS \geq ds_1 \mid EDP = edp] = \max\left\{ \Phi\left(\frac{\ln edp - \ln \theta_{c,1}}{\beta_{c,1}}\right), \Phi\left(\frac{\ln edp - \ln \theta_{c,2}}{\beta_{c,2}}\right) \right\} \tag{8}$$

The results of the IDA and the approximated curves by the bilinear regression analysis are presented in Figure 6, where safety factor is set as 1.2. The IDA plots express the mean probability of exceedance for given $IM_{rel} = im$. Note that the approximation curves are discontinuous at $IM_{rel} = im^* = 23$ cm for SH model and 14 cm for HH model due to the change of $\theta_{DS|IM}$ and $\beta_{DS|IM}$ before and after the point of im^* [Tubaldi et al. 2016]. From this figure, the impact of using different seismic performance levels and different adjacent buildings on the vulnerability of expansion joints can be compared. The left side in Figure 6 shows the results of SH model, whereas the right side shows the results of HH model. Each figure contains the IM_{rel} values corresponding to the seismic hazard levels of 43-year, 72-year, and 475-year return period at Tokyo. These hazard levels are often considered in performance-based design framework [Hadijian A 2002] and the 475-year level is usually set as the target seismic hazard for seismic pounding analysis [CEN 2005, BCJ 2008]. In this study, the target seismic hazard to ensure the safety of the expansion joints is set as the 72-year level. The derivation procedure for these IM_{rel} values is presented in Section 6.

Compared between SH model and HH model, it is evident that the expansion joints installed on HH model have a significantly lower probability of exceedance in the range of $IM_{rel} > im^*$ due to the in-phase motions of the two buildings induced by the structural yielding. This fact indicates that the expansion joints installed on similar two buildings which tend to behave similarly in the nonlinear range than in the linear range may suffer from slight damage, but the failure of those expansion joints is unlikely to occur. For example, against the 72-year seismic hazard level, the SD expansion joints installed on HH model become in DS1 with the probability of more than 50%, but the failure probability is only less 20%. In the case of the HP expansion joints on HH model, even the probability of being in DS1 is quite low because of their high seismic performances. In summary, the safety factor of 1.2 can be sufficient for the HP and SD expansion joints installed on HH model to ensure their functions against the 72-year hazard level.

The expansion joints installed on SH model are more vulnerable than those installed on HH model because the in-phase motions of the two buildings were not much observed. For the HP expansion joints, the probability of being in DS1 against the 72-year hazard is less than 40% and thus the safety factor of 1.2 is recommended. This is not the case for the SD expansion joints due to the less seismic capacities compared with the HP expansion joints. For the SD expansion joints, the probability of being in DS1 against the 72-year hazard exceeds 90%. Especially for the SD wall expansion joints, the failure probability exceeds 70% and the safety factor of 1.2 is insufficient to ensure its function. Therefore, the next section discusses the recommended SF to ensure the function of the SD expansion joints installed on SH model.

5.5 Failure probability of SD expansion joints on SH model with different safety factors

Figure 7 shows the probabilities of the two failure states, "SD floor Failure" and "SD wall Failure", for the expansion joints installed on SH model with the safety factors of 1.2, 1.5, and 1.8. Note that SF in the figures stand for safety factor. In general, the increase of the safety factor from 1.2 to 1.5 or from 1.5 to 1.8 results in 20% decrease of the failure probability. For the SD floor expansion joints in Figure 7(a), the recommended safety factor can be set as 1.5 because the failure probability against the 72-year hazard is decreased to within 10%. For the SD wall expansion joints, however, the safety factor of 1.5 still has the failure probability of 40% against the 72-year level and the safety factor of 1.8 is recommended.

To summarize this section, it was demonstrated that the building characteristics affect the selection of the performance level and safety factor of expansion joints. For adjacent buildings showing the in-phase behavior in the inelastic range, the use of the expansion joints with lower seismic performance such as the SD expansion joints can be accepted. In contrast, when the fundamental periods of two buildings are different, the in-phase motion is not apparent in the inelastic range. In this case, the expansion joints with higher seismic performance such as the HP expansion joints are recommended. If the clearance and safety factor can be extended enough, the SD expansion joints are good design option.

6   COST-EFFECTIVE SELECTION OF EXPANSION JOINTS

6.1   Concept

Under the current design practice, the selection of expansion joints and the associated safety factors is not based on quantitative information and vaguely determined by structural designers and building owners. It is also difficult to compare the expected life-cycle costs of various expansion joints in consideration due to the lack of fragility and repair cost information. In contrast to the current situation, building owners want to make an economic selection in consideration of seismic performance level, initial cost, expected loss, expected downtime, and so on. Several studies proposed a cost-effective design method where the optimal design is the one that gives the minimum life-cycle cost [Wen et al. 2001, Liu et al. 1993, Yanaka et al. 2016]. Following this concept, this section demonstrates the selection procedure of the expansion joint that gives minimum life-cycle cost. Figure 8 describes the procedure.

At the first step in Figure 8, the seismic pounding risk analysis of adjacent buildings is performed and the minimum level of clearance and safety factor is determined. The next step is to select expansion joints to be installed between adjacent buildings. For each expansion joint under consideration, fragility function and information on initial cost and repair cost are obtained. The expected annual loss (EAL) (= expected annual repair cost) of expansion joints is then calculated by the following integrations [Deierlein GG et al. 2003]:

$$EAL = \sum_{i=1}^{n} E(C_R \mid ds_i) \int_{im} P(ds_i \mid im) \mid dv(im) \mid \tag{9}$$

where $E(C_R|ds_i)$ is the expected repair cost C_R of expansion joints given $DS = ds_i$, obtained from [Otsuki et al. 2018a], $P(ds_i|im)$ is the probability of being in $DS = ds_i$ given $IM = im$ obtained from Eq. (7), and $v(im)$ is the mean annual frequency of exceedance of $IM = im$. Finally, the expected life-cycle cost $LC(t)$ over the target lifespan t years is obtained by:

$$LC(t) = EAL \cdot t + C_I \tag{10}$$

where C_I is the initial cost of expansion joints. The optimal selection of the expansion joints and the safety factor is finally achieved by comparing the calculated life-cycle costs for several expansion joints.

6.2   Case study

This section performs case studies to select the cost-effective expansion joint and its safety factor for the adjacent building models. The procedure follows those described in Figure 8. Suppose that a structural designer and a building owner are concerned with which expansion joints should be installed and what extent of the safety factor should be considered for SH model and HH model. The available options are the sets of the HP expansion joints or SD expansion joints. Each set consists of one floor and two wall expansion joints of the tested HP and SD expansion joints. The location of buildings is at Tokyo, where the minimum separation distance between two buildings is calculated based on the Japanese Level 2 design spectrum. As same in Section 5, the safety factor of 1.2, 1.5, and 1.8 are considered here and the corresponding motion ranges are those in Table 5. The selection of the HP or SD expansion joint sets and the safety factors with least life-cycle cost is investigated. Note that the consequence of failures is not considered in this study.

6.2.1   Seismic pounding analysis

The likelihood of the seismic pounding occurrence between adjacent buildings was first evaluated to determine the minimum level of the safety factor. The seismic pounding considered for SH model and HH model means the earthquake-induced collision between the end of sky bridges and one end of building surface. Several procedures for probabilistic assessment of seismic pounding are proposed by [Tubaldi et al. 2012, Barbato and Tubaldi 2013], but a simple evaluation is conducted here. At first, seismic hazard curve which expresses $v(im)$ in Eq. (9) for IM_{rel} for the locations of buildings, Tokyo, is created. Architectural Institute of Japan (AIJ) [AIJ 2016] provides uniform hazard spectra that express spectral acceleration for each period for four different hazard levels (50%, 10%, 5% and 2% in 50 years) with 5% damping ratio. The corresponding IM_{rel} values of four hazard levels for each adjacent building model were then calculated by Eq. (5) after the modification of spectra values by 1.5 / (1+0.1h), where h is the damping ratio of each model. The seismic hazard curves were obtained by performing hyperbolic approximation described in [Bradly et al. 2007]. Figure 9(a) shows the obtained seismic hazard curves for SH model and HH model. The probability of seismic pounding occurrence given $IM = im$ is then expressed by [Tubaldi et al. 2016]:

$$P[u_{rel} \geq \xi \mid IM = im] = \begin{cases} \Phi\left(\dfrac{\ln a_1 + b_1 \ln im - \xi}{\beta_{EDP|IM}}\right) & IM = im \leq im^* \\[2em] \Phi\left(\dfrac{\ln a_1 + (b_1 - b_2)\ln im^* + b_2 \ln im - \xi}{\beta_{EDP|IM}}\right) & IM = im > im^* \end{cases} \tag{11}$$

where u_{rel} is the peak relative displacement, ξ is the clearance between two buildings as listed in Table 5, and $\ln a_1$, b_1, b_2, $\ln im^*$, and $\beta_{EDP|IM}$ are those obtained by the bilinear regression.

Figure 9(b)-(c) shows the probability of seismic pounding with various safety factors obtained by using Eq. (11). The target seismic hazard to avoid the seismic pounding is set as 475-year return periods (10% in 50 years), which is nearly equivalent to the one in [CEN 2005, BCJ 2008]. For SH model in Figure 9(b), the consideration of the safety factor of 1.2 is insufficient because the seismic pounding occurs with the probability of 40% against the 475-year seismic hazard level. Therefore, it is recommended to have at least the safety factor of 1.5 where the probability of seismic pounding is less than 20% against the 475-year level. In the case for HH model in Figure 9(c), the seismic pounding does not occur even with the minimum level of SF =1.0, which allows us select wide range of expansion joints. In summary, the minimum level of the safety factor of each adjacent building model is determined in consideration of seismic pounding risk, which is 1.5 for SH model and 1.0 for HH model.

6.2.2 *Seismic loss assessment of expansion joints*

Structural designers gather fragility functions and cost information of building components and calculate life-cycle cost. The life-cycle cost of building components is usually calculated as the sum of the initial cost, repair or replacement cost, cost for people's injury, and loss of profits due to the loss of building service [Takahashi et al. 2004]. There is a possibility that people get injured by the falling of expansion joints and business service on a certain floor or area stops due to the failure of expansion joints, but the analysis here does not consider the loss associated with the consequence of damage because data is not available. For cost calculation, the inflation rate is ignored and thus, the life-cycle cost is defined simply as the sum of the initial cost and expected loss (or expected repair cost). When further information are obtained in future earthquakes, the loss assessment analysis presented herein should be improved.

Fragility functions used here are those developed in this paper. The initial cost of expansion joints can be divided into the initial material cost C_M and initial construction cost for installation C_C.

$$C_I = C_M + C_C \tag{12}$$

It is known that both C_M and C_C increase as the increase of the motion range due to the increase of the materials and complexity in construction. According to the expansion joint manufacturer who joined our shaking table tests, as the increase of the motion range by 10 cm, the material cost increases approximately 40% for the tested HP expansion joints and 20% for the tested SD expansion joints. The construction cost increases approximately 30% for the HP and SD expansion joints. In the experiment, the motion range of the expansion joints was 17.5 cm, and the material cost was 695000JPY ($US6950) for the set of the HP expansion joints and 405000JPY ($US4050) for the set of the SD expansion joints. The construction cost for each set was 300000JPY ($US3000). Therefore, in this case study, the following formula is used to estimate the material cost and construction cost for the sets of the HP and SD expansion joints for arbitrary motion ranges:

$$C_{M(HP)} = 695000 \times 1.4^{(D_{exp}-17.5)/10}$$

$$C_{M(SD)} = 405000 \times 1.2^{(D_{exp}-17.5)/10} \tag{13}$$

$$C_C = 300000 \times 1.3^{(D_{exp}-17.5)/10}$$

where $C_{M(HP)}$ and $C_{M(SD)}$ are the material cost for the sets of the HP and SD expansion joints, respectively. C_C is the construction cost for installation. D_{exp} is the motion range of the expansion joints with unit of centimeter.

Information on repair cost of the expansion joints is obtained from [Otsuki et al. 2018a], where the expected repair cost $E(C_R|ds_i)$ for given damage state $DS = ds_i$ is expressed as the ratio to the initial cost:

$$E(C_R \mid ds_i) = r\ (ds_i) \cdot C_I = r_M\ (ds_i) \cdot C_M + r_C(ds_i) \cdot C_C \tag{14}$$

where $r_M(ds_i)$ and $r_C(ds_i)$ are the ratio of repair cost for material and construction to the initial cost for material and construction, respectively.

Using Eq. (9), EAL of each set of the expansion joints is calculated as shown in Figure 10. Compared between the HP and SD expansion joints, EAL of the HP expansion joints is significantly smaller than that of the SD expansion joints because of the different seismic capacities. Compared between SH model and HH model, HH model has lower EAL due to the in-phase motion of the two buildings in the range of large IM_{rel} values. For all cases, a larger SF reduces EAL. However, the larger SF results in the increase of the initial cost. Therefore, the recommend safety factor with the least life-cycle cost is evaluated in the next section.

6.2.3 *Comparison of life-cycle cost*

Figure 11 shows the relationship between the lifespan and expected life-cycle cost (= initial cost + expected loss) calculated by Eq. (10). The slope of each line corresponds to EAL in Figure 10. Here we select the optimal expansion joints and SF by assuming the 50-year lifespan. For SH model in Figure 11(a), the optimal selection seems the HP expansion joints with SF = 1.2 or the SD expansion joints with SF = 1.8. However, recall that SF = 1.2 cannot be allowed due to the high possibility

of seismic pounding and the SD expansion joints with SF = 1.8 are the optimal choice. For HH model in Figure 11(b), the optimal selection is the SD expansion joints with 1.5 or 1.8. For both cases, alternative selection can be made depending on decision maker's interests such as the lower damage probability with use of the HP expansion joints considering the continuity of building service, the lower risk of seismic pounding with use of a larger safety factor or depending on design/construction limitations of the installation location.

The relationship of SF and expected life-cycle cost considering the 50-year lifespan is presented in Figure 12. For SH model in Figure 12(a), the minimum level of the safety factor is 1.5 considering the seismic pounding risk. Thus, the HP expansion joints cannot be the optimal selection and the SD expansion joints with the safety factor of 1.8 is the best choice. For HH model, the minimum safety factor is taken as 1.0 and the SD expansion joints with the safety factor of 1.5 is the optimal choice. In the case that a large safety factor cannot be taken due to the limitation of the installation place, the HP expansion joints with the safety factor of 1.0 can be a good alternative choice.

In summary, the selection procedure of expansion joints with use of the developed fragility functions and repair cost information was demonstrated. In consideration of seismic pounding risk, vulnerability, and expected seismic loss of expansion joints, decision makers can decide the performance level and safety factor of expansion joints. The results showed that the selection of expansion joints for adjacent buildings differs with building characteristics that affect the relationship between the peak relative displacement and IM_{rel} especially in inelastic range. It was also demonstrated that the alternative selection of expansion joints can be made by changing the performance level and safety factor depending on the decision maker's interests. The presented information can be useful as a reference for designers and building owners in the selection of expansion joints.

7   CONCLUSIONS

This study conducted a vulnerability and seismic loss assessment of expansion joints. Four commonly used expansion joints, high-performance (HP) and standard (SD) for floor and wall, were investigated. Their motion range was 50% of the clearance between adjacent buildings. The clearance between adjacent buildings is set by assuming safety factor multiplying the peak relative displacement against a target seismic hazard. The considered adjacent buildings in this study were two types, SH model (55-story Super high-rise and 13-story High-rise) and HH model (13-story High-rise and 13-story High-rise). At first, the displacement-dependent fragility functions of the expansions joints were developed based on the previous shaking table tests. The vulnerability of the expansion joints installed on the adjacent building models was evaluated by incremental dynamic analysis and the constructed fragility functions. In the end, an idea of cost-effective selection of expansion joints was presented and case studies were conducted for the considered adjacent building models. The major findings are summarized as follows:

1. Fragility functions of the HP and SD expansion joints for floor and wall were proposed. Because damage to expansion joints mainly depends on the peak relative displacement, the dispersion of the fragility functions was determined in consideration of the initial position errors expected in expansion joints. The median value was taken from the critical length in the drawings and from the experimental results. Considering the nature of displacement-dependency, fragility functions of other types of expansion joints should be constructed from their drawings by identifying the critical length and expected initial position errors as assumed in this paper.

2. The difference in the component-level seismic vulnerability between the HP and SD expansion joints is evident. The probability of the HP expansion joints being in damage state 1 within the design motion range is less than 20%, whereas it is more than 60% for the SD expansion joints. The probability of failure for the SD expansion joints increases rapidly immediately after the motion range.

3. The building characteristics affect the selection of expansion joints. For adjacent buildings showing the in-phase behavior in the inelastic range such as HH model, the use of the expansion joints with lower seismic performance or a smaller safety factor can be accepted. Thus, for HH model, a smaller safety factor such as 1.2 can be sufficient to ensure the function of the HP and SD expansion joints. On the contrary, the in-phase motion of the two buildings is not apparent for SH model where the fundamental periods are largely different. This result demands the safety factor of 1.5 or more for the SD expansion joints on SH model.

4. The benefits of the presented selection procedure of expansion joints with use of fragility information compared with the current practice are that 1) the decision making is firmly based on quantitative information on the vulnerability and cost of expansion joints and 2) the alternative selection of expansion joints such as different performance levels and safety factors can be made at the desired performance level and the design/construction limitations.

5. Case studies were performed to select the expansion joints for SH model and HH model to demonstrate the above benefits. Considering the high seismic pounding risk for SH model, the optimal selection in terms of life-cycle cost was determined as the SD expansion joints with the safety factor of 1.8. In contrast, the probability of seismic pounding for HH model was quite low, which enables us several options. The optimal selection was the SD expansion joints with the safety factor of 1.5 and the HP expansion joints with the safety factor of 1.0 can be a good alternative option in case that the extending the clearance and safety factor is difficult.

The results confirmed that the characteristics of adjacent buildings affected the selection of expansion joints. This is because the relationship between the peak relative displacement and the intensity measure changes when buildings become inelastic range. Thus, the tendency of the peak relative displacements of various types of buildings over wide range of the intensity measure will be investigated as a future work. Moreover, many fragility and repair cost estimations of expansion joints is required to further cultivate the presented selection procedure.

ACKNOWLEDGMENTS

REFERENCES

1. Sullivan, T.J., Arifin, F.A., MacRae, G.A., Kurata, M., Takeda, T. "Cost-Effective Consideration of Non-Structural Elements: Lessons from the Canterbury Earthquakes," 16th European Conference on Earthquake Engineering, June 18-21, 2018.
2. Skalomenos KA, Hatzigeorgiou GD, Beskos DE. Modelling level selection for seismic analysis of concrete-filled steel tube/moment resisting frames by using fragility curves. *Earthquake Engineering and Structural Dynamics*. 2015; 44(2): 199-220
3. Federal Emergency Management Agency (FEMA). P-58 Next-generation Seismic Performance Assessment for Buildings, Volume 1 – Methodology, FEMA, Washington, D.C., USA, 2012.
4. Architectural Institute of Japan (AIJ), Report on the Damage Investigation of the 2005 West off Fukuoka Earthquake, Tokyo, 2005. (in Japanese)
5. National Institute for Land and Infrastructure Management (NILIM)and Building Research Institute (BRI). Quick Report of the Field Survey on the Building Damage by the 2016 Kumamoto Earthquake. Technical Note of NILIM No. 929 and Building Research Data No. 173, Tokyo, JAPAN, 2016. (in Japanese)
6. Kasai K, Mita A, Kitamura H, Matsuda K, Morgan T, Taylor A. Performance of Seismic Protection Technologies during the 2011 Tohoku-Oki Earthquake. *Earthquake Spectra*. 2013; 29(1): 265-293.
7. Bertero V V. Observations of structural pounding. Proceedings of the International Conference on the Mexico Earthquake 1985: Factors Involved and Lessons Learned; September 19-21, 1986; Mexico City, Mexico.
8. Filiatrault A, Cervantes M, Folz B, Prion H. Pounding of buildings during earthquakes: a Canadian perspective. Canadian Journal of Civil Engineering. 1994; 21(2): 251-265.
9. Kasai K, Maison B F. Building Pounding Damage During the 1989 Loma Prieta Earthquake. *Engineering Structures*. 1997; 19(3): 195-207.
10. Public Works Research Institute (PWRI), Report on the disaster caused by the 1995 Hyogoken Nanbu Earthquake. *Journal of Research*. 1997; 33.
11. Cole L G, Dhakal P R, Turner M F. Building pounding damage observed in the 2011 Christchurch earthquake. Earthquake Engng Struc Dyn. 2012; 41: 893-913.
12. Architectural Institute of Japan, Tohoku branch (AIJ), Report on the disaster caused by the 2011 Tohoku Earthquake. 2013. (in Japanese)
13. Japanese Society of Seismic Isolation (JSSI). Guideline on Expansion Joints for Seismic Isolation buildings. JSSI, Tokyo, JAPAN, 2013. (in Japanese)
14. Japan Expansion Joint Association (JEJA). Guideline of Expansion Joints for Buildings. JEJA, Tokyo, JAPAN, 2016. (in Japanese)
15. Building Center of Japan (BCJ). Criteria for Structural Calculation for Buildings Split by Expansion Joints, Building letter, 2008; 506. (in Japanese)
16. International Conference of Building Officials (ICBO). Uniform Building Code. ICBO, Whittier, CA, USA, 1997.
17. European Committee for Standardization (CEN). *European Standard EN 1998-1: 2005 Eurocode 8: Design of structures for earthquake resistance. Part 1: General rules, Seismic action and rules for buildings*. European Committee for Standardization: Brussels, Belgium, 2005.
18. Construction and Planning Administration Ministry of Interior. *Seismic Provisions*. Building Code (TBC): Taipei, Taiwan, 1997.
19. Tubaldi E, Freddi F, Barbato M. Probabilistic seismic demand model for pounding risk assessment. *Earthquake Engineering & Structural Dynamics.* 2016; 45(11): 1743–1758.
20. Architectural Institute of Japan (AIJ). Recommendation for Aseismic Design and Construction of Nostructural Elements. AIJ, Tokyo, 2003. (in Japanese)

21. Otsuki Y, Kurata M, Skalomenos K, Ikeda Y. Damage sequence and safety margin assessment of expansion joints by shake table testing. 2018a. (under the revision)

22. Porter K, Kennedy R, Bachman R. Creating Fragility Functions for Performance-Based Earthquake Engineering. *Earthquake Spectra*. 2007; 23(2): 471–489.

23. Japanese Society of Seismic Isolation (JSSI). Maintenance and Management Standards for Isolation Building. JSSI, Tokyo, 2010. (in Japanese)

24. Kasai K, Jagiasi A, Jeng V. Inelastic vibration phase theory for seismic pounding mitigation. *Journal of Structural Engineering*. 1996; 122(10): 1133-1146.

25. Tubaldi E, Barbato M. Probabilistic risk analysis of structural impact in seismic events for linear and nonlinear systems. *Earthquake Engineering & Structural Dynamics*. 2015; 44(3): 491–493.

26. Otsuki Y, Buyco K, Kurata M, Speicher M. Feasibility Study on Multi-code Seismic Evaluation of a Landmark Building. Proceedings of the 11th National Conference in Earthquake Engineering, Earthquake Engineering Research Institute, Los Angeles, CA. 2018b.

27. Lin J, Weng C. Probability analysis of seismic pounding of adjacent buildings. *Earthquake Engineering & Structural Dynamics*. 2001; 30(10): 1539–1557.

28. Pacific Earthquake Engineering Research Center (PEER). Open System for Earthquake Engineering Simulation (OpenSees) Framework, University of California, Berkely, available at http://opensees.berkeley.edu/.

29. Akiyama H. P-δ Effect in Earthquake Resistant Design for Shear Type Multi-story Frames. *Journal of Structure and Construction Engineering*. 2007; 617: 87-94. (in Japanese)

30. Vamvatsikos D, Cornell A. Incremental dynamic analysis. *Earthquake Engineering & Structural Dynamics*. 2002; 31(3): 491–514.

31. Biasio M, Grange S, Dufour F, Allain F, Petre‐Lazar I. Intensity measures for probabilistic assessment of non‐structural components acceleration demand. *Earthquake Engineering & Structural Dynamics*. 2015; 44(13): 2261‐2280.

32. Jeng V, Kasai K, Maison BF. A spectral difference method to estimate building separations to avoid pounding. *Earthquake Spectra*. 1992; 8(2):201–223.

33. Federal Emergency Management Agency (FEMA). P-695 Quantification of Building Seismic Performance Factors, FEMA, Washington, D.C., 2009.

34. Pacific Earthquake Engineering Research Center (PEER). Strong Motions Database, University of California, Berkeley, available at http://ngawest2.berkeley.edu/ [last access February 2017].

35. Baker JW, Cornell, CA, 2005. Vector-Valued Ground Motion Intensity Measures for Probabilistic Seismic Demand Analysis, Report No. 150, John A. Blume Earthquake Engineering Center, Stanford, CA, 321 pp.

36. Baker JW, Jayaram N, Shahi S. Ground motion studies for transportation systems, 2011. available at http://peer.berkeley.edu/transportation/projects/ground-motion-studies-for-transportation-systems/ [last access February 2017].

37. Padgett J, Nielson B, DesRoches R. Selection of optimal intensity measures in probabilistic seismic demand models of highway bridge portfolios. *Earthquake Engineering & Structural Dynamics*. 2008; 37(5).

38. Wen YK, Kang YJ. Minimum building life-cycle cost design criteria. II: Applications. 2001. *Journal of Structural Engineering*. 2001; 127(3): 338-346.

39. Liu M, Burns S, Wen. Optimal seismic design of steel frame buildings based on life cycle cost considerations. *Earthquake Engineering & Structural Dynamics*. 2003; 32(9): 1313–1332.

40. Yanaka M, Ghasemi S, Nowak A. Reliability‐based and life‐cycle cost‐oriented design recommendations for prestressed concrete bridge girders. *Structural Concrete*. 2016; 17(5): 836‐847.

41. Deierlein GG, Krawinkler H, Cornell CA. A framework for performance-based earthquake engineering. Proceedings of the 2003 Pacific Conference on Earthquake Engineering.

42. Tubaldi E, Barbato M, Ghazizadeh S. A probabilistic performance-based risk assessment approach for seismic pounding with efficient application to linear systems. *Structural Safety*. 2012; 36: 14–22.

43. Barbato M, Tubaldi E. A probabilistic performance‐based approach for mitigating the seismic pounding risk between adjacent buildings. *Earthquake Engineering & Structural Dynamics*. 2013; 42(8): 1203‐1219.

44. Architectural Institute of Japan (AIJ). Guidebook of Recommendations for Loads on Buildings, Maruzen. 2016. (in Japanese)

45. Bradley B, Dhakal R, Cubrinovski M, Mander J, MacRae G. Improved seismic hazard model with application to probabilistic seismic demand analysis. *Earthquake Engineering & Structural Dynamics*. 2007; 36(14): 2211–2225.

46. Takahashi Y, Kiureghian A, Ang A. Life-cycle cost analysis based on a renewal model of earthquake occurrences. *Earthquake Engineering & Structural Dynamics*. 2004; 33(7): 859‐880.
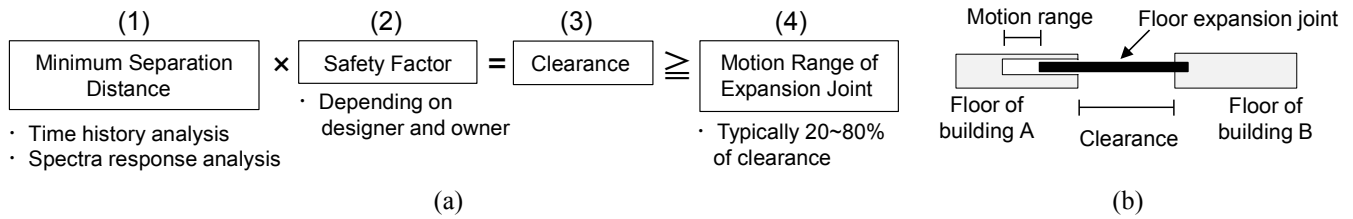
(a)

(b)

Figure 1 Overview of expansion joints: (a) Seismic design of expansion joints and (b) definition of clearance and motion range for a typical floor expansion joint
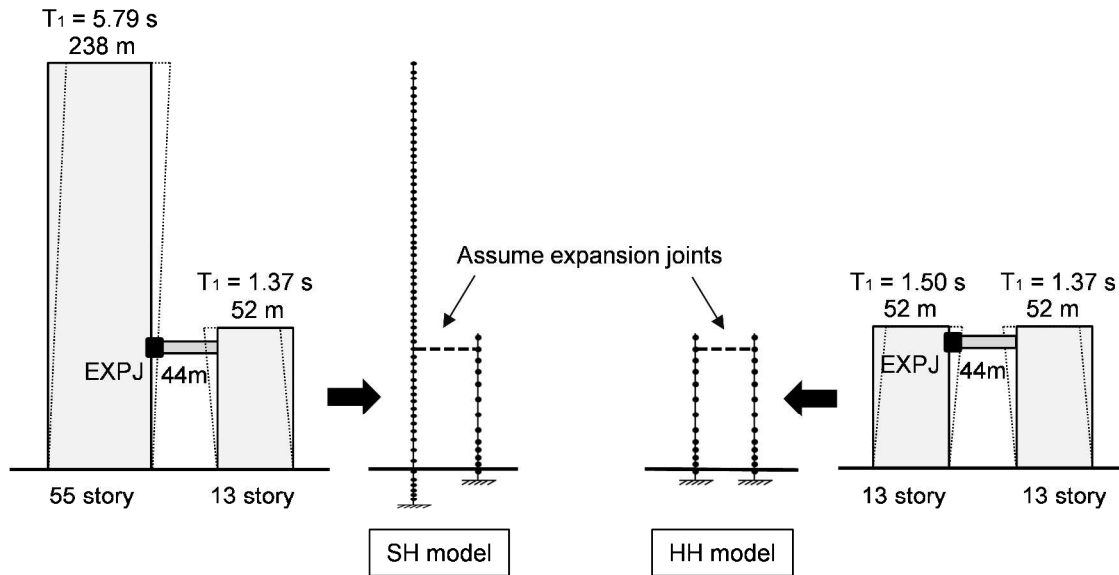

Figure 2 Adjacent building models where expansion joints were assumed at a height of 44 m
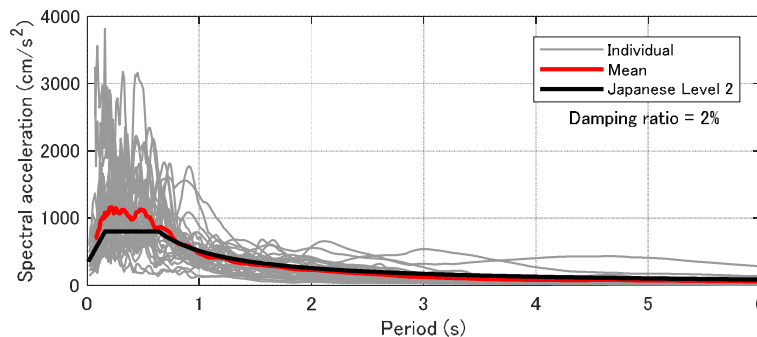

Figure 3 Acceleration response spectra of 30 ground motions with the Japanese Level 2 design spectrum with 2% damping ratio
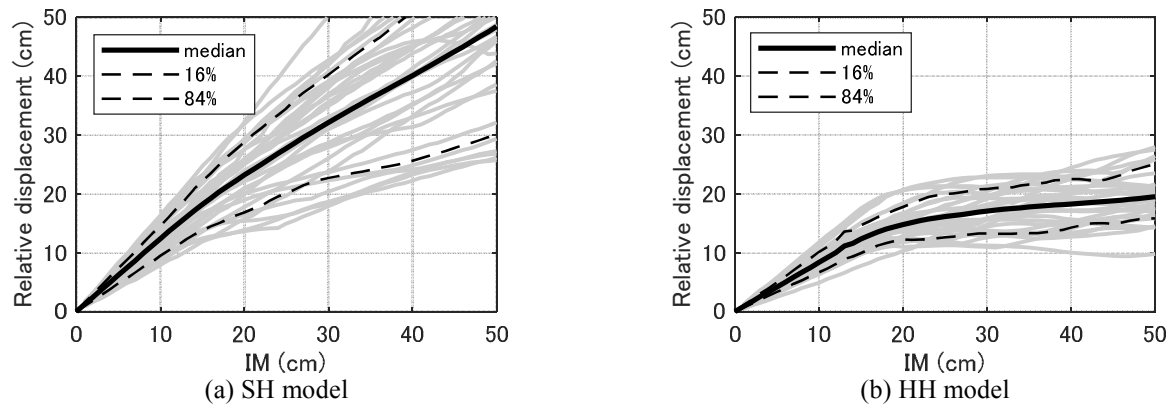
(a) SH model   (b) HH model

Figure 4 IDA curve for IM_{rel} - peak relative displacement relationship

(a)   (b)
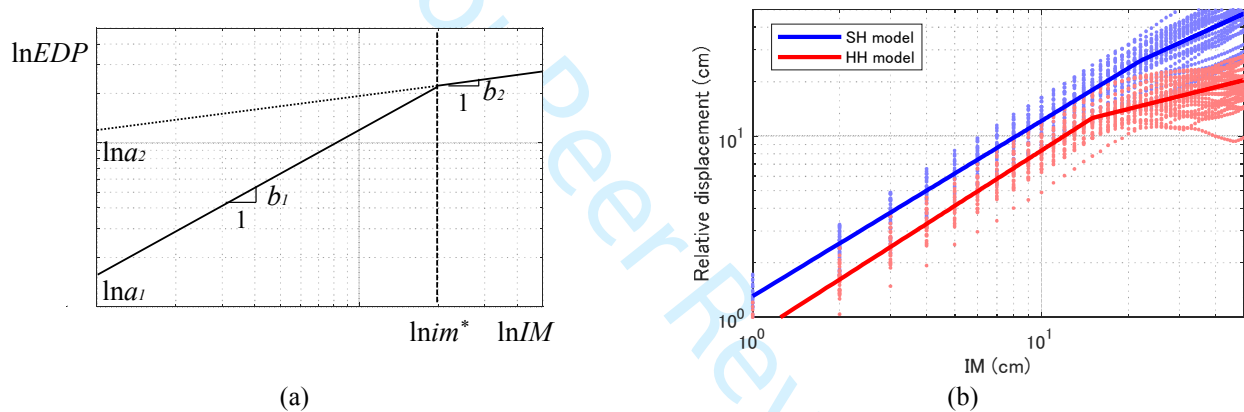
Figure 5 Bilinear regression analysis: (a) regression parameters and (b) regression curves for IDA results
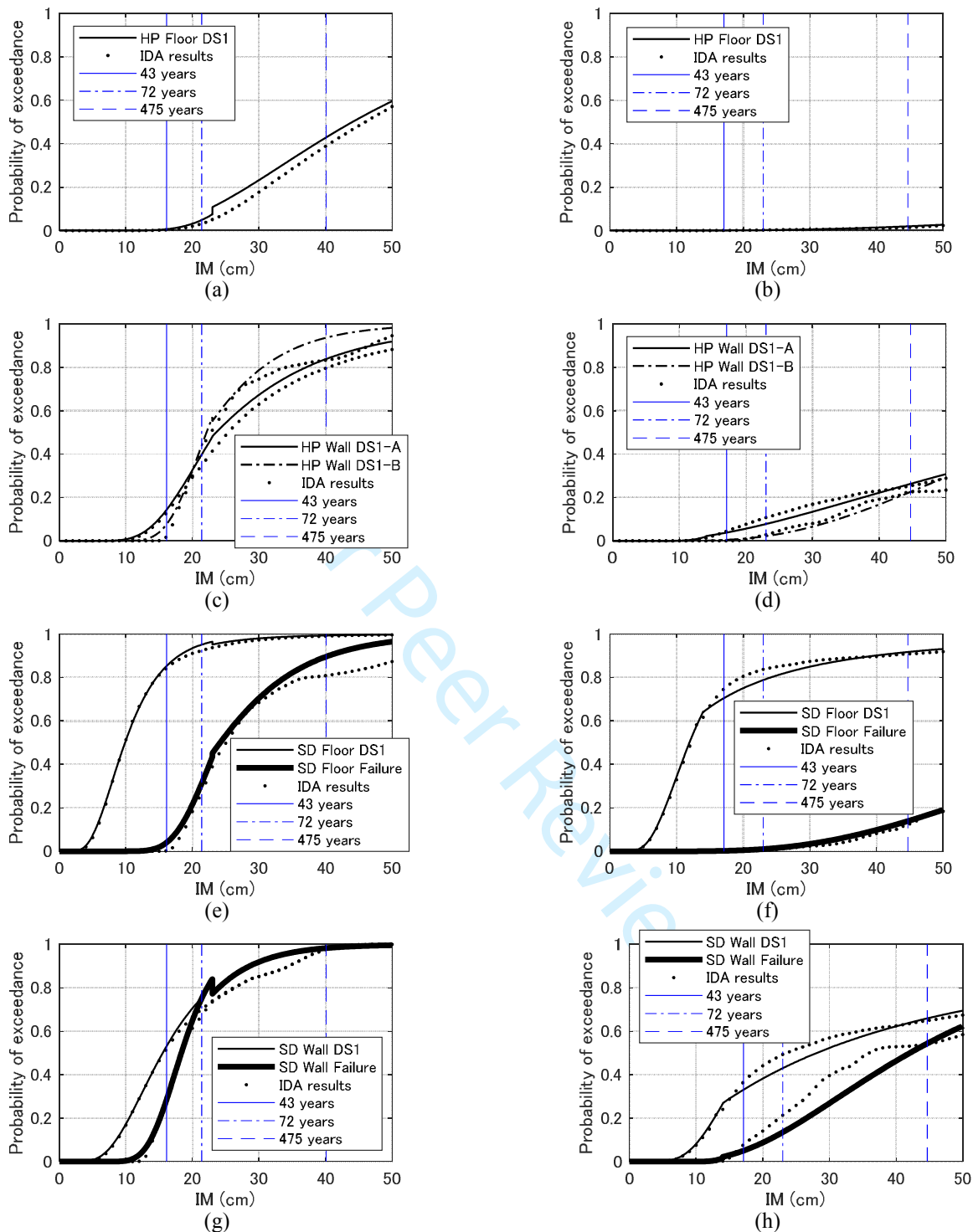
Figure 6 **Probability of exceedance of each damage state when safety factor is 1.2 (left side is for SH model and right side is for HH model): (a)-(b) HP floor DS1, (c)-(d) HP wall DS1-A and DS1-B, (e)-(f) SD floor DS1 and failure, and (g)-(h) SD wall DS1 and failure**
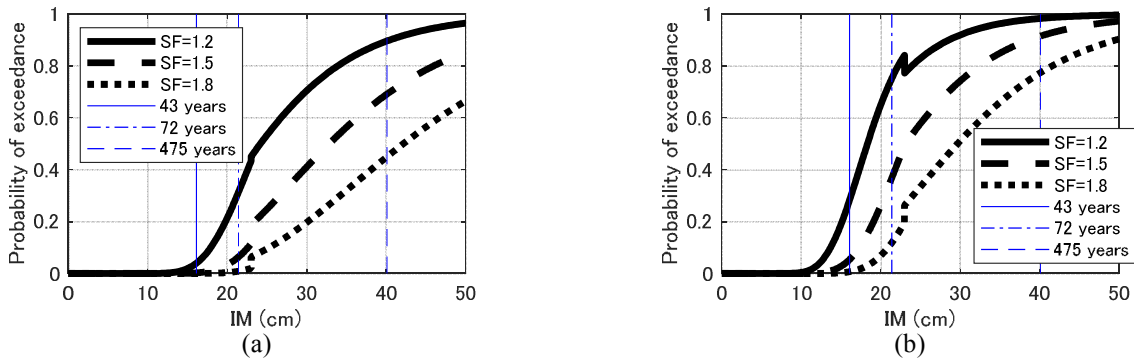
Figure 7 Probability of exceedance of failure state of SD expansion joints installed on SH model when Safety factor are 1.2, 1.5 and 1.8: (a) SD floor failure and (b) SD wall failure.
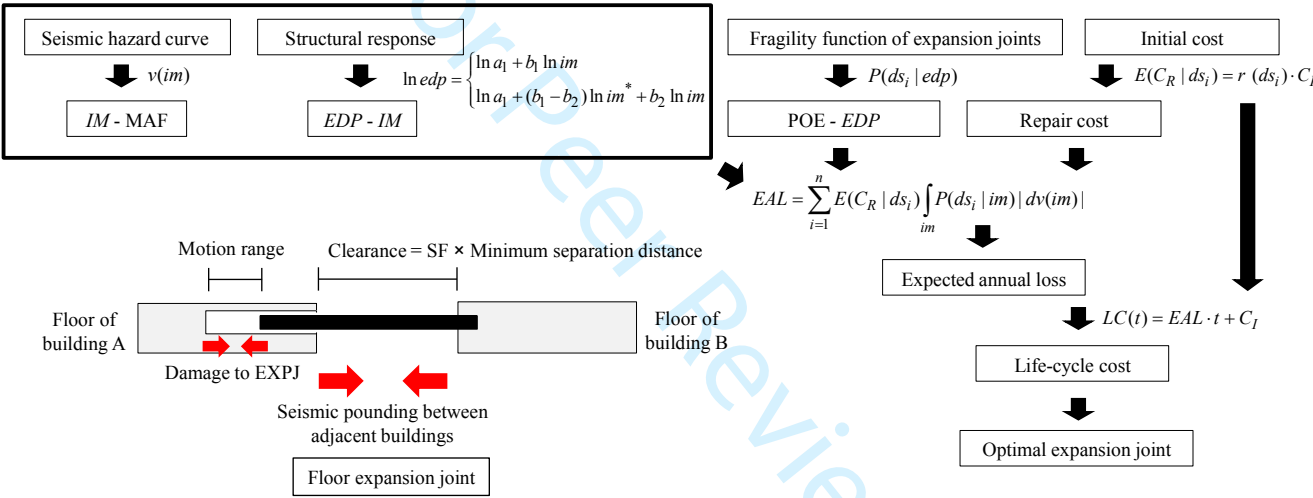
Figure 8 Flow of cost-effective selection of expansion joints
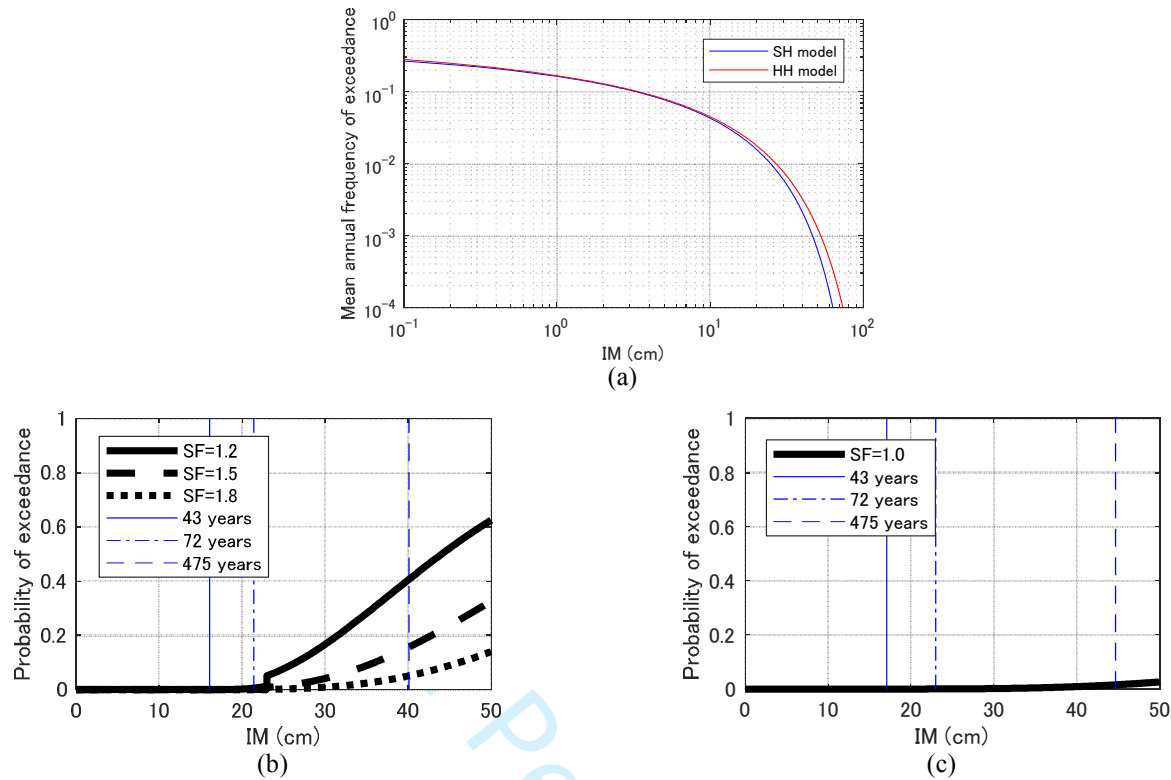
Figure 9 Seismic pounding risk assessment with various safety factors: (a) seismic hazard curve for IM_{rel}, (b) probability of seismic pounding for SH model and (c) for HH model
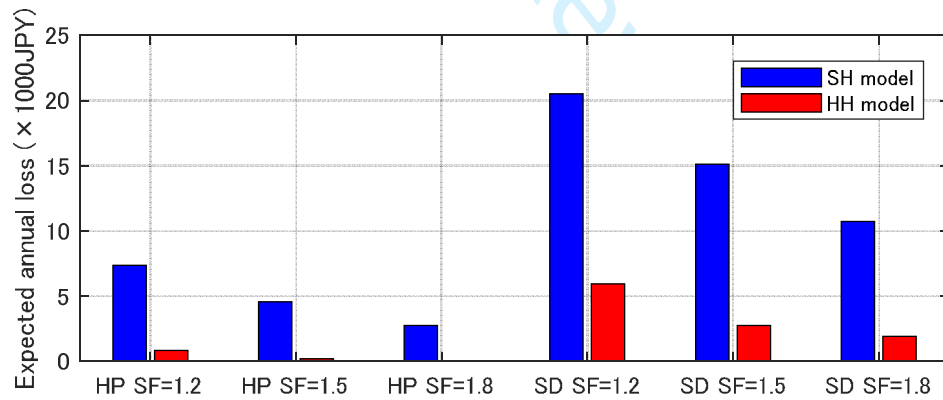
Figure 10 Expected annual loss for each expansion joint and safety factor

Earthquake Engineering and Structural Dynamics

(a)

(b)
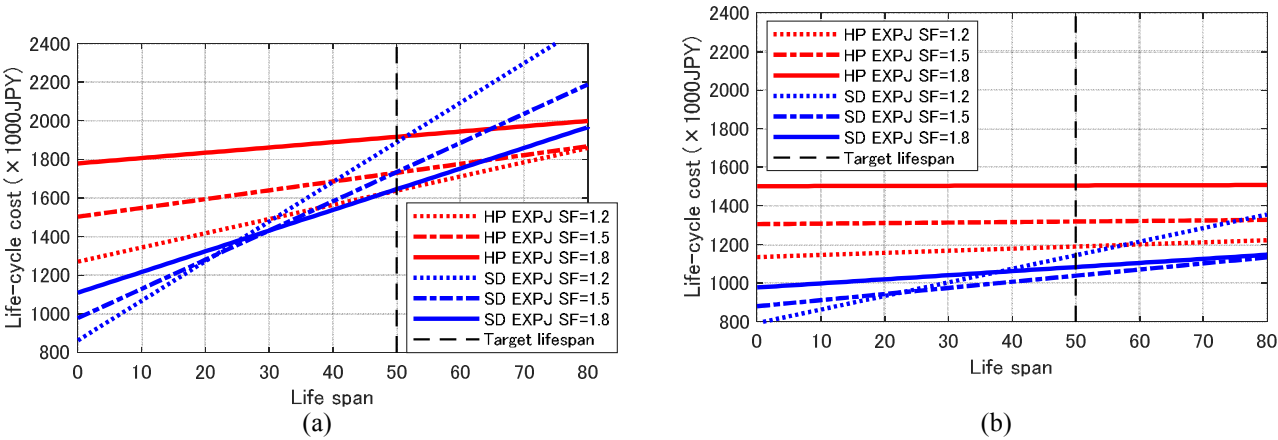
Figure 11 Sum of the initial cost and expected loss of expansion joints vs lifespan: (a) SH model and (b) HH model

(a)

(b)
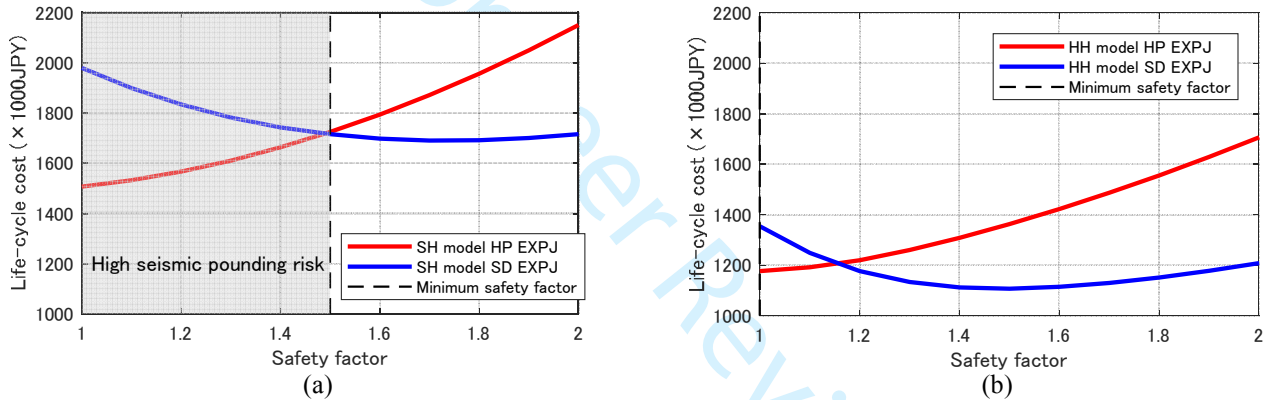
Figure 12 Sum of the initial cost and expected loss of expansion joints vs safety factor for the 50-year lifespan: (a) SH model and (b) HH model

Table 1 Summary of tested expansion joints and damage states [Otsuki et al. 2018]
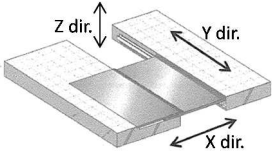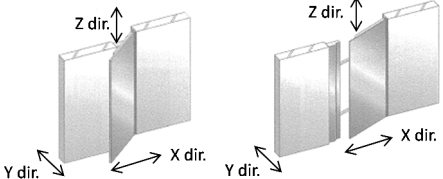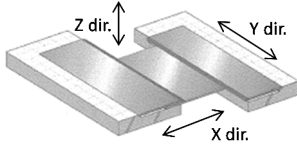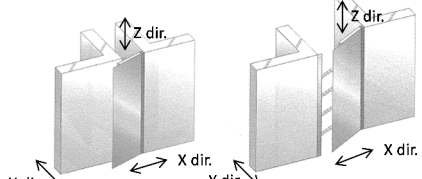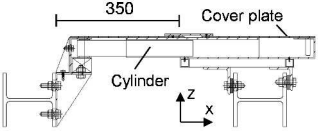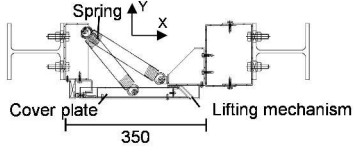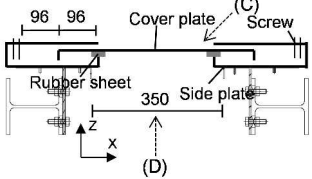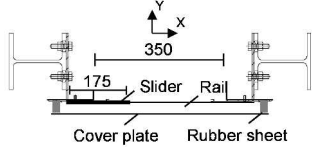
	High-performance floor expansion joint	High-performance wall expansion joint		Standard-performance floor expansion joint		Standard-performance wall expansion joint	
Deformation mechanism	 Sliding type	 Lifting type		 Sliding type		 Sliding type	
Drawing							
Damage state	DS1 Cove Plate Relocated	DS1-A Spring Deformation	DS1-B Screw Rupture	DS1 Screw Rupture	Failure Cover Plate Disengaged	DS1 Rubber Sheet Disengaged	Failure Cover Plate Dropped Off
Damage description	Cover plate was disengaged due to collisions with other components. Cover plate can be easily fixed by relocating it to the original position.	Totally three of five springs had residual deformations after a collision with other component.	Screws were fractured due to the impact force applied when collisions occurred.	Drill screws were bent and ruptured due to several collisions with the cover plate.	Cover plate was disengaged from the side plate, creating a gap between floors.	Rubber sheets were disengaged, creating a gap that led to concern about air and water leakage	Cover plate fell off because its sliders railed off.
Critical relative displacement (ratio to the motion range of 17.5 cm)	33.8 cm (193%)	19.1 cm for one spring and 23.6 cm for the other two springs (109% and 132%)	20.3 cm (116%)	9.4 cm (54%)	22.2 cm (127%)	— (Due to rubbing with other components)	17.6 cm for the front wall and 19.0 cm for the back wall (101% and 109%)

Table 2 Initial position errors expected in expansion joints (unit: cm) [JSSI 2010]

	HP expansion joints	SD expansion joints
Construction	±2.0	±2.0
Dry expansion and contraction	±1.0	±1.0
Heat expansion and contraction	±0.5	±0.5
Residual displacement	±1.0	±3.0
Total standard deviation by assuming 3σ = sum of the above maximum values	$\sigma_{HP} = \sqrt{\left(\dfrac{2.0}{3}\right)^2 + \left(\dfrac{1.0}{3}\right)^2 + \left(\dfrac{0.5}{3}\right)^2 + \left(\dfrac{1.0}{3}\right)^2}$ $= 0.83$	$\sigma_{SD} = \sqrt{\left(\dfrac{2.0}{3}\right)^2 + \left(\dfrac{1.0}{3}\right)^2 + \left(\dfrac{0.5}{3}\right)^2 + \left(\dfrac{3.0}{3}\right)^2}$ $= 1.26$

Table 3 Fragility functions of expansion joints with design motion range D_{expj} of 17.5 cm
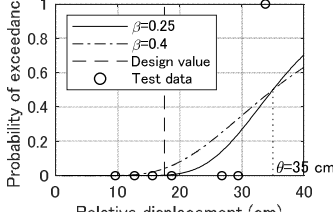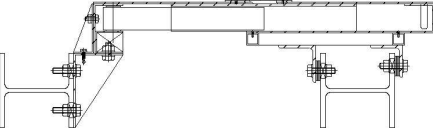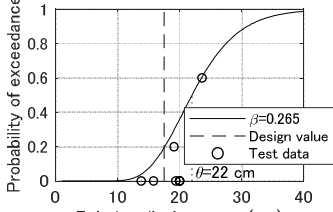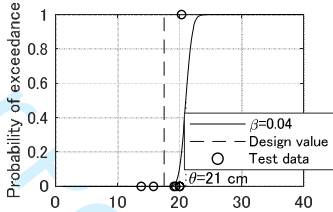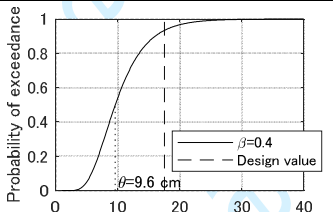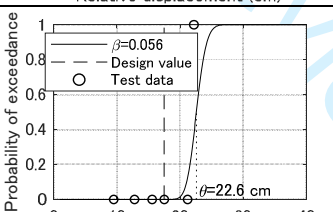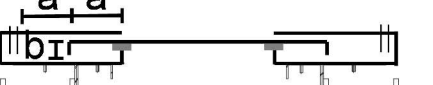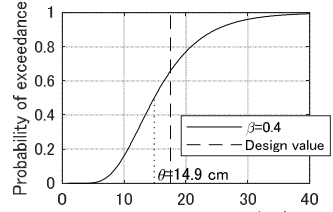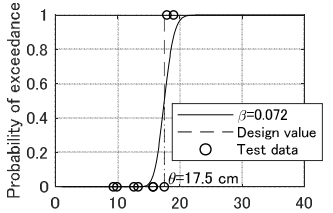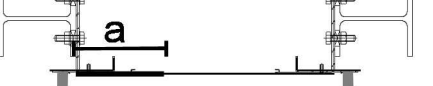
HP floor expansion joint **DS1: Cover plate relocated** $\theta_{c,i} = 2.0D_{expj} = 2.0 \times 17.5 = 35.0$ cm $\beta_{c,i} = 0.250$		
HP wall expansion joint **DS1-A: Spring deformation** $\theta_{c,i} = 22.0$ cm $\beta_{c,i} = 0.265$		
HP wall expansion joint **DS1-B: Screw rupture** $\theta_{c,i} = a = 21.0$ cm $\beta_{c,i} = \dfrac{\sigma_{HP}}{\theta_{c,i}} = \dfrac{0.83}{21.0} = 0.040$		
SD floor expansion joint **DS1: Screw rupture** $\theta_{c,i} = a = 9.6$ cm $\beta_{c,i} = 0.400$		
SD floor expansion joint **Failure: Cover plate disengaged** $\theta_{c,i} = 2(a+b) = 2(9.6+1.7) = 22.6$ cm $\beta_{c,i} = \dfrac{\sigma_{SD}}{\theta_{c,i}} = \dfrac{1.26}{22.6} = 0.056$		
SD wall expansion joint **DS1: Rubber sheet disengaged** $\theta_{c,i} = 0.85D_{expj} = 0.85 \times 17.5 = 14.9$ cm $\beta_{c,i} = 0.400$		
SD wall expansion joint **Failure: Cover plate dropped** $\theta_{c,i} = a = 17.5$ cm $\beta_{c,i} = \dfrac{\sigma_{SD}}{\theta_{c,i}} = \dfrac{1.26}{17.5} = 0.072$		

Table 4 Experimental results for damage of springs [Otsuki et al. 2018]

Input amplitude of sinewave 1Hz (cm/s^2)	Maximum relative displacement on the compression side r_i (cm)	Total of damaged springs n_i of 5 springs
300	13.8	0
350	15.8	0
400	19.1	1
450	19.4	0
500	20.0	0
550	20.0	0
600	23.6	3

Table 5 Clearance and motion range of expansion joints installed on each model

Model	IM_{rel} for Japanese Level 2 spectrum (cm) (1)	Safety factor (SF) (2)	Clearance between adjacent buildings (cm) = (1)×(2)	Motion range of expansion joints (cm) = (1)×(2)×0.5
SH model	36.5	1.2	43.8	21.9
		1.5	54.8	27.4
		1.8	65.7	32.9
HH model	30.4	1.2	36.5	18.3
		1.5	45.6	22.8
		1.8	54.7	27.4

Table 6 Estimation parameters for Eq. (6)

	$IM = im \leq im^*$	$IM = im > im^*$
$\ln edp \mid im$	$\ln a_1 + b_1 \ln im$	$\ln a_1 + (b_1 - b_2)\ln im^* + b_2 \ln im$
$\beta_{EDP\mid IM}$	$\sqrt{\dfrac{\sum_{k=1}^{N_1}(\ln edp_k - (\ln a_1 + b_1 \ln im_k))^2}{N_1 - 2}}$ N_1 = number of simulation cases in $IM = im \leq im^*$	$\sqrt{\dfrac{\sum_{k=1}^{N_2}(\ln edp_k - (\ln a_1 + (b_1 - b_2)\ln im^* + b_2 \ln im_k))^2}{N_2 - 2}}$ N_2 = number of simulation cases in $IM = im > im^*$
$\beta_{DS\mid IM}$	$\dfrac{\sqrt{\beta_{EDP\mid IM}^2 + \beta_{c,i}^2}}{b_1}$	$\dfrac{\sqrt{\beta_{EDP\mid IM}^2 + \beta_{c,i}^2}}{b_2}$
$\ln \theta_{DS\mid IM}$	$\dfrac{\ln \theta_{c,i} - \ln a_1}{b_1}$	$\dfrac{\ln \theta_{c,i} - (\ln a_1 + (b_1 - b_2)\ln im^*)}{b_2}$